12.5-m distance mesurement in high-interference environment Using ultrasonic array Sensors

Yukiko Yoshikawa
Graduate School of Science, Technology and Innovation
Kobe University
Kobe, Japan
yoshikawa.yukiko@cs28.cs.kobe-u.ac.jp

Yuto Yasuda
Department of Computer Science and Systems Engineering
Kobe University
Kobe, Japan
yasuda.yuto@cs28.cs.kobe-u.ac.jp

Ishii Toru
Graduate School of Science, Technology and Innovation
Kobe University
Kobe, Japan
ishii.toru@cs28.cs.kobe-u.ac.jp

Shintaro Izumi
Graduate School of System Imformatics
Kobe University
Kobe, Japan
shin@godzilla.kobe-u.ac.jp

Hiroshi Kawaguchi
Graduate school of Science, Technology and Innovation
Kobe University
Kobe, Japan
kawapy@godzilla.kobe-u.ac.jp

Abstract— We presents distance measurement technique in high-interference environment using ultrasonic array sensors and direct sequence spread spectrum. First, this paper explains time of flight calculation methods for enhancing the reflected waves from the object. Then, results obtained using this method are discussed. Object detection in an environment with much interference can be achieved with machine learning. Evaluation results show that the proposed method can measure the distance of static target in range of 2-12.5 m ± 5 cm (99% accuracy) and a target moving at 0-2.0 m/s in range of 2-7 m ± 30 cm (77% accuracy). We also conducted 3D measurement that was able to detect an object in outdoor at 11 m.

Keywords—Ultrasound, DSSS, Doppler shift, Beamforming

I. Introduction

Ultrasonic measurement technology has attracted attention for decades. Various ultrasonic applications in robotics and security have been developed in recent years. Ultrasonic distance imaging system can recognize a position. Beamforming techniques for distance image acquisition are of particular interest and an ultrasonic transmitter array (UTA) is used for this purpose. In contrast to Lidar [1] and optical methods, ultrasonic imaging systems present great benefits in term of privacy in monitoring activities. In general, measuring the distance of an object from a distance image is done using the time of flight (TOF) [2-11].

However, ultrasonic waves undergo great attenuation of acoustic signal in air. For that reason, several studies been done to address this issue. The use of spread-spectrum techniques is known to improves noise resistance and increase the measurement range [6]. Using the techniques, a transmitter consisting of four arrays with eight elements has been reported as able to measure distance images over a range of 6 m [7]. In addition, simulation have shown that ultrasonic array transmitter driving higher power with an increased number of elements can improve the sound pressure and directivity [8]. Earlier reports have described the use of those techniques: an ultrasonic distance sensing system with 144 elements and a high voltage of 30 Vpp can measure up to 50 m [9], and another sensing system with 64 elements and voltage of 20 Vpp can acquire the distances of two objects at 0.5-6 m [10]. Because these studies are conducted in an anechoic room in which no other reflection waves exist, useful ultrasonic imaging systems in the environment of reflected waves from surrounding environment must be considered.

In this study, we implement a UTA using sixteen ultrasound transducers with a fundamental frequency of 25 kHz and a voltage of 60 Vpp, and discuss how to process reflected waves from surrounding environment. We also used MEMS microphones for the receiver array to minimize element spacing [11]. By correcting the reflected signal, we achieved the 1D measurement of a static object and a dynamic object according to changes in their location. Using machine learning, we could demonstrate that classification was possible. To demonstrate the possibility of classifying objects in 3D distance images, we measured the position of a static object in an environment of reflect waves.

II. Theory

Fig. **1** presents a schematic diagram of our ultrasonic signal processing system. All received signals stored by the recorder are computed on the PC.

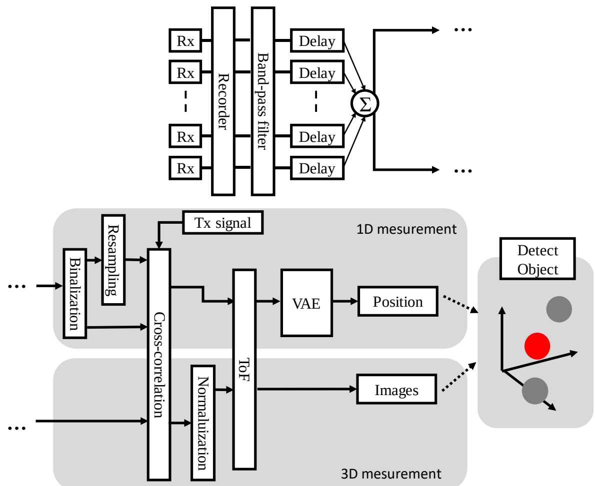

Fig. 1. Diagram of ultrasonic measurement system.

This paper is based on results obtained from a project commissioned by the New Energy and Industrial Technology Development Organization (NEDO).

A. *Distance measurement of static object using DSSS*

As described in reports of earlier studies, a direct sequence spread spectrum (DSSS) signal using the M-sequence or other similar codes is noise resistant making it particularly useful for distance measurements. The method of estimating the TOF is determination of a point that shows the highest peak of cross correlation between the reflected wave and the known transmission sequence using DSSS: the magnitude of the correlation value is proportional to the similarity and sound pressure of the received signal. The propagation loss of ultrasonic method is large. Therefore, if non-target objects are closer to receiver than the object, the distance attenuation should be considered when classifying the peaks. Using our method, the decrease of the peak value with distance is suppressed by making the amplitude uniform through binarization of the received signal. The binarization is given by the following equation for static objects:

$$x_r(t) = \begin{cases} 1\ (x_r(t) > x_c) \\ -1 (x_r(t) < x_c) \end{cases} \tag{1}$$

where x_r represents the received signal, and x_c is a mean power of microphone outputs.

B. *Distance measurement of dynamic object using DSSS*

For a dynamic object, because of the Doppler shift, the main peak becomes less noticeable as the velocity increase. Reportedly, the speed limit depends on the DSSS code length [12], derived from the number of waves per bit and the bit length. For this study, we used to a 32-bit signal with eight wavelengths per bit for accurate measurements, which is less affected by the narrow bandwidth of the UTA device. The peak can be detected using the resampled transmission sequence for cross-correlation according to Doppler speed if the peak cannot be detected beyond the limit speed. The resampling ratio is represented by the following formula:

$$(vs - vd)/vs \tag{2}$$

where vd is the object's velocity, and vs is the acoustic wave speed in air.

C. *3D position and shape recognition by beamforming*

Beamforming enables us to measure an object in three dimensions. The amount of delay given to each element for beamforming is given by the following equation:

$$\Delta t_n = dy_n \sin(\theta) \cos(\varphi) + dz_n \sin(\theta) \sin(\varphi) \tag{3}$$

Therein, the array is in the Y-Z plane; the output direction is shown by the X axis. dy_n and dz_n are the distances of n-th elements from the center of the array, where θ represents the arrival angle around the X axis and φ from the Y-Z plane.

Similarly, detecting the peaks at a distance is important also for 3D measurements. The received signal is calculated by adding the delayed signals in equation (3), which needs a liner summation. Therefore, the method of detecting the far-field peaks by binarization is inappropriate. The received signal power Pr from a uniformly radiating spherical waves from speakers is given by the following equation:

$$Pr = \frac{Pt}{4\pi R^2} \tag{4}$$

where, Pt stands for peak transmitter power, R expresses the distance from the speaker. Based on this equation (4), we multiply the correlation value by R^2 to enable us to detect the peaks at greater distances.

III. Experimental Results

A. *Transmitter and receiver*

Fig. 2 (a) shows the developed UTA, ultrasonic receiver array (URA) and other setups used for the experiment. The UTA comprises sixteen transducers (MSO-AT1625H12T: Changzhou Manorshi Electronics Co. Ltd. with 16.2-mm diameter) and mutual element spacing of 17 mm. Each transducer is driven at 60 Vpp, with a fundamental frequency of 25 kHz. The URA consists of sixteen MEMS microphones (SPU0410LR5H-QB: Knowles Electronics, the dimension is 3.76 mm,) which allows for short element spacing of 7mm. By shortening the element space to less than the half-wave length of the transmitted signal, the side lobe effect can be reduced. Using the parameters of the developed sensors, we computed their synthesized directivity by computer simulation; Fig. 2 (b) shows the UTA, UTR, and synthesized one whose main lobe azimuth angle is peakier around 0°.

The transmit signal was a 32-bit long code with eight waves per bit, generated by a digital pattern generator (410-338, Digital Discovery; Digilent Inc.). The received signal was amplified by an operational amplifier and was captured synchronously with the transmitted signal at a sampling frequency of 1MHz using a data recorder (MR6000; HIOKI E.E. Corp). To demonstrate the effectiveness of our method, we conducted experiments in a room with much interference from various sources.

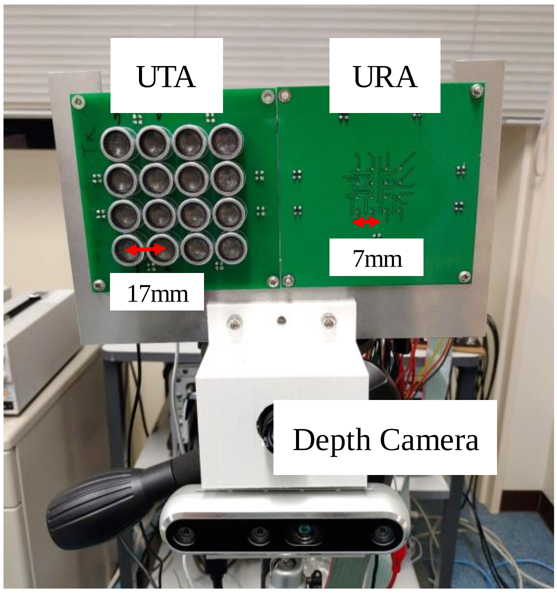

(a)

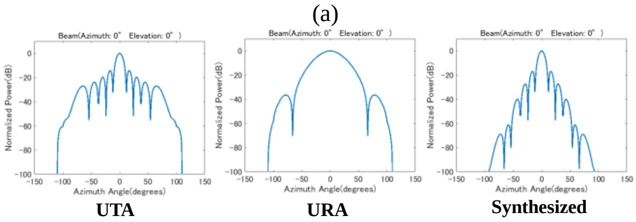

(b)

Fig. 2. (a) Sensors and (b) direction characteristics of UTA, URA, and synthesized one.

B. 1D static evaluation

We used a circular plate with a 1-m diameter as the object, as shown in Fig. **3**. The sensor is placed at 1.2 m from the floor on the horizontal line in the center of the circular plate. Two hundred measurements were taken at 18 fixed positions from 4.0 m to 12.5 m (at every 0.5 m step). We binarized all signals. Fig. **4** shows that the binarization suppresses the decrease in the correlation value with distance. We can distinguish the circular plate that are standing at 12.5 m, which has stronger signals than the non-binarization case at a long distance.

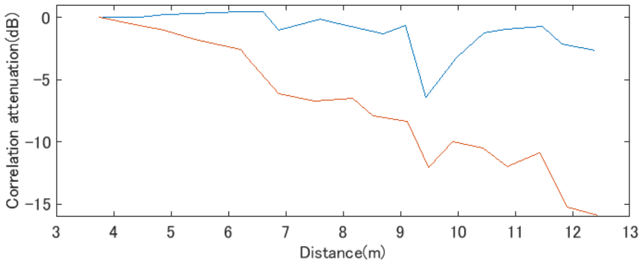

Fig. 5 shows the signal intensity in the correlation peak of an object depending on the distance. In the non-binarization experiment, the correlation peaks signal decrease by 15 dB at 12.5 m, while that is 2 dB in the binarization experiment.

Fig. 3. Circular plates for static and dynamic experiments.

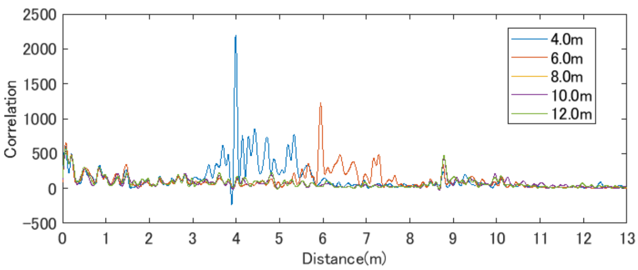

(a)

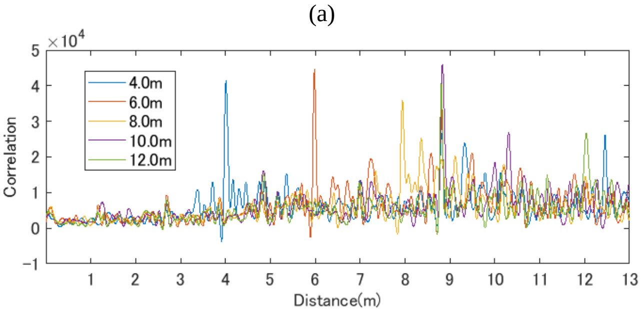

(b)

Fig. 4. Comparison of (a) non-binarization and (b) binarization in 1D static experiments.

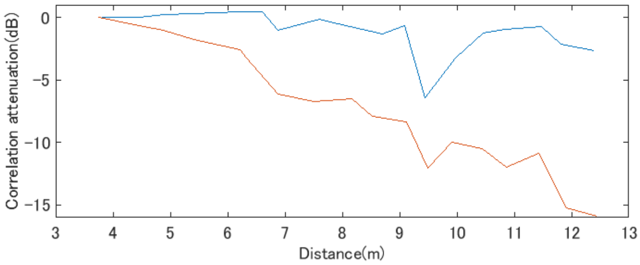

Fig. 5. Signal compensation by binarization.

We adopt a variable auto encoder (VAE) as machine learning, which can extract common features from data. It finds the peaks of an object from multiple peaks that contain ambient signals. Fig. 6 (a) shows the VAE learning method. The correlation values, normalized pulse, were trained as the training data. Correlation values with peaks only at the location of the object were trained as correct data. Out of the 3,116 measurement data obtained, 2,587 training data and 529 validation data were trained. Consequently, as shown in Fig. 6 (b), we were able to detect the peak of the object from the correlation values under high-inference indoor environment. The percentage of correct answers was 99% in 150 epochs, allowing an error of ± 5 cm.

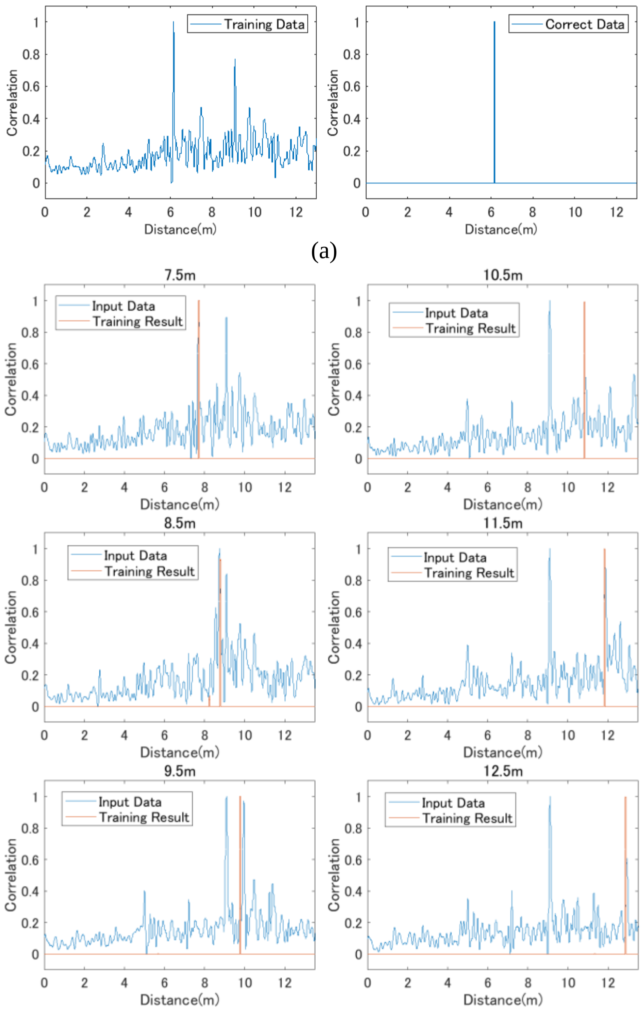

(a)

(b)

Fig. 6. Machine Learning with VAE for static measurement: (a) an example dataset and (b) inference results.

C. 1D Dynamic evaluation

The left picture in Fig. **3** (b) presents the environment used for dynamic experiment. We held the circular plate in our hands and moved the object in direction where the Doppler velocity was negative. The walking state from 4 m to 5 m is saved at one-second intervals.

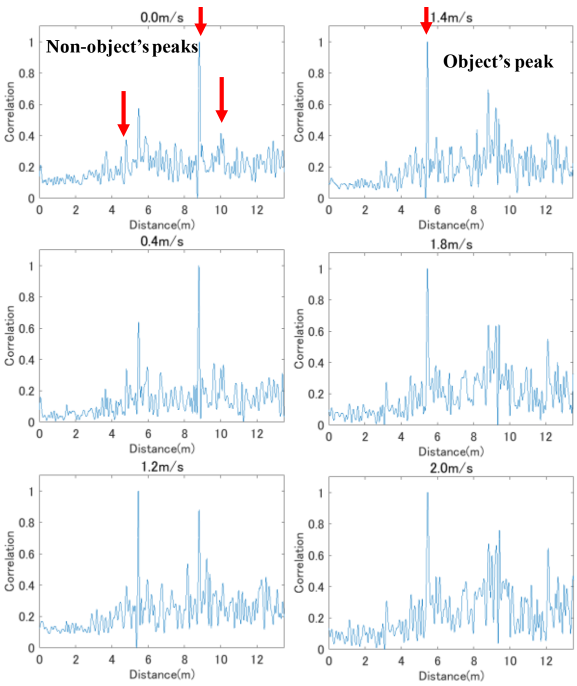

Fig. 7 shows the cross-correlation between the reflected waves of moving object and the resampled transmission sequence with the Doppler velocity varied by every 0.1 m/s. In the figure, the closer is to the object's velocity of 1.2 m/s.

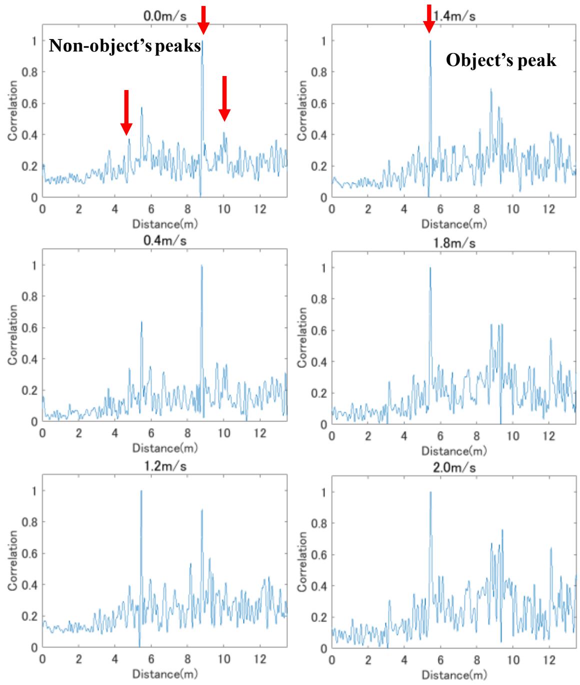

Fig. 7. Correlation values of the dynamic object and non-target objects with Doppler compensation.

We measured 1,982 data, and then all were binarized: 21-series correlations were calculated using the transmission sequences resampled from 0.0 m/s to 2.0 m/s. Fig. 8 (a) shows the learning method used for the VAE in dynamic experiment. The correct distances were acquired using a depth camera. A teacher signal was expressed in the form of normal distribution curb. We used 1,734 data (× 21 datasets) for learning data and the rest 194 data for test data. The training results are shown in Fig. 8 (b). The percentage of correct answers in a range of 2-7m was 77% in 1000-epoch training, allowing for an error of ± 30 cm.

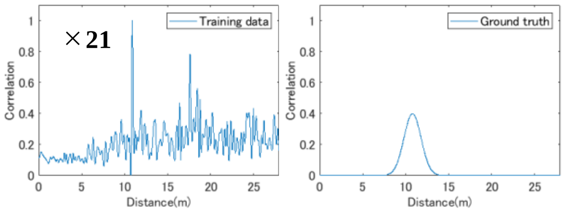

(a)

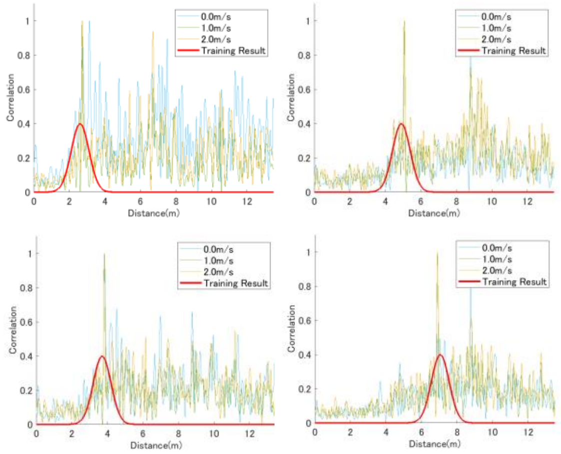

(b)

Fig. 8. Machine Learning with VAE for dynamic measurement: an example dataset and (b) inference results.

D. 3D static evaluation

For 3D evaluation, we carried out outdoor experiment. We detected the same circular plate as shown in Fig. **3** by directing the transmitter beam to both elevation and azimuth angles of 0°, where the target locations has three cases (center, left and right around ± 12°). The distance from the transmitter to the plate at each location is slightly different due to the outdoor experimental environment. Fig. 9 shows visualization of the correlation values of which distance and azimuth angle in vertical and horizontal axis, respectively. The distance and angle of the object detected is the area with the highest correlation value. The object at each different position can be detected. TABLE I presents a comparison with the actual distance measured using the range finder.

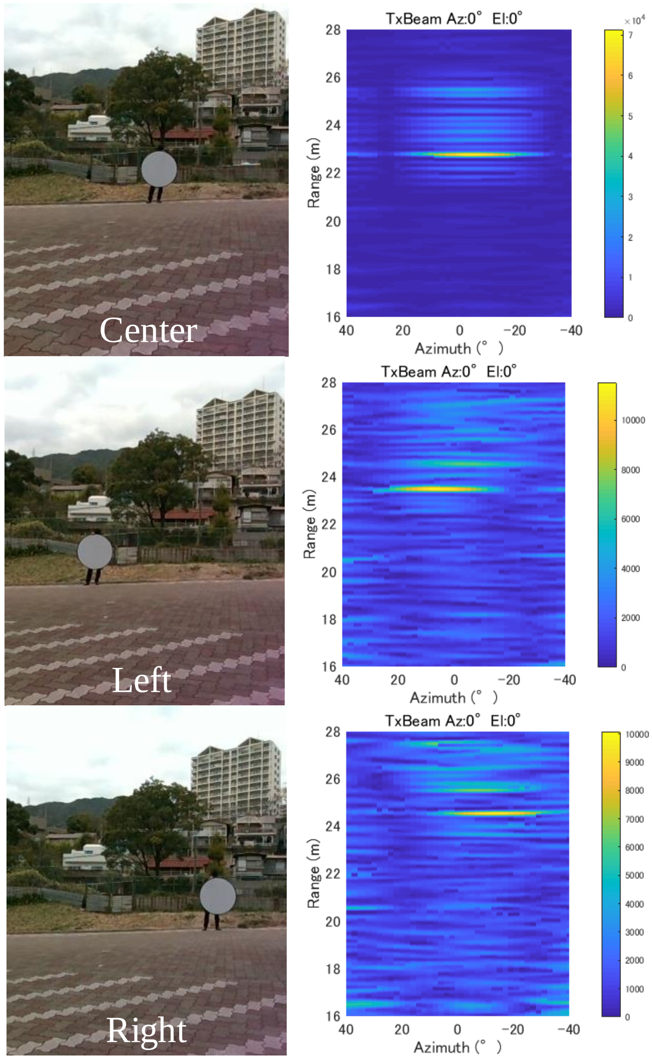

Fig. 9. Visualization of 3D measurement in outdoor.

TABLE I. 3D outdoor measurement (azimuth 0°, elevation 0°)

Position	Correct		Measurement	
	Distance (m)	Angle (°)	Distance (m)	Angle (°)
Center	22.78	0.0	22.77	−2
Left	23.58	11.9	23.49	7
Right	24.73	−12.4	24.55	−12

As well, we conducted another experiment in the room with higher interference. Referring to Fig. 2, the beamforming scan width of the UTA was found as -24° to 24° azimuth. We took measurements from 24° to -24° azimuth by every 3° step at elevation of -5° We used a narrow 1.2 m × 0.4 m wooden board as the object and installed it at 4-m distance (center, left and right by 0.5 m). Fig. 10 the measurement results, and TABLE II presents a comparison with the actual distance measured using the range finder. In a room with many reflections from surrounding environment, the detectable range is shorter, but we were able to detect the object.

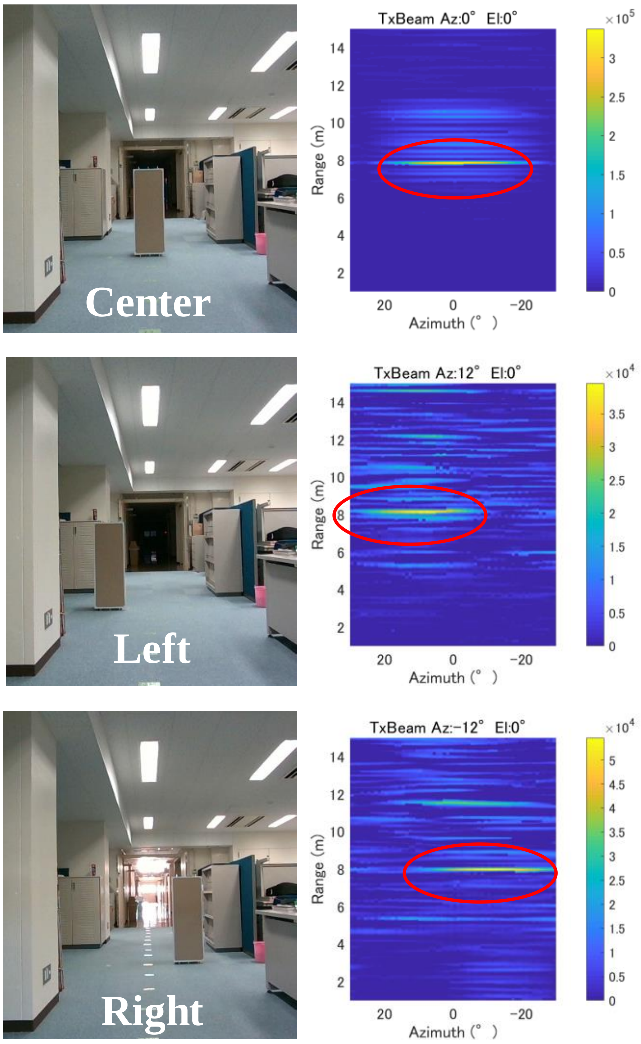

Fig. 10. The results of 3D measurement in the room.

TABLE II. 3D indoor measurement (elevation −5°)

Position (azimuth)	Correct		Measurement	
	Distance (m)	Angle (°)	Distance (m)	Angle (°)
Center (0°)	7.73	0.0	7.86	−1
Left (12°)	8.04	7.4	8.16	9
Right (−12°)	7.83	−9.6	7.95	−12

IV. Conclusion

A method with ultrasonic DSSS was proposed for measuring objects using UTA consisting of 16 ultrasound transducers and URA consisting of 16 MEMS microphones. For 3D ranging, we were able to detect object at 22.7 m outdoor and at 7.8 m in the room, a static valuation. In static distance measurement, we could distinguish objects on the beam and measure 12.5 m ± 5 cm distance with 99% accuracy. For 0-2m/s dynamic evaluation, 2-7 m ± 30 cm were possible with 77% accuracy. TABLE III summarizes comparison with conventional range imaging techniques.

TABLE III. Comparison with conventional methods.

	Proposed	[9]	[10]
Number of elements	16	144	64
Noiseless environment	11 m (outdoor)	25 m (anechoic room)	3 m (anechoic room)
Indoor environment	12.5 m (static) 7.0 m (dynamic)	N/A	N/A

[1] R. Whyte, L. Streeter, L. Cree, and M. J. Cree, "Appliocation of Lider Technique to Time-of-Flight Range Imaging," *OSA Applied Optics*, vol. 54, no. 33, pp. 9654-9664, Nov. 2015.

[2] P. N. Keating, T. Sawatari, and G. Zilinskas, "Signal processing in acoustic imaging," *Proceeding of the IEEE*, vol. 67, no. 4, pp. 496-510, Apr. 1979.

[3] J. D. Dvorak, M. L. Stone, and K. P. Self, "Object Detection for Agricultural and Construction Environments Using an Ultrasonic Sensor," *Journal of Agricultural Safety and Health*, vol. 22, no. 2, pp. 107-119, Apr. 2016.

[4] S. Harput, and A. Bozkurt "Ultrasonic Phased Array Device for Acoustic Imaging in Air," *IEEE Sensours Jurnal*, vol 8, no. 11, pp.1755-1762, Nov. 2008.

[5] H. Furuhashi, Y. Kuzuya, Y.Uchida, and M. Shimizu, "Three dimentional imaging sensor system using an ultrasonic array sensor and a camera," *Proceedings of IEEE SENSORS*, pp. 713-718, Nov. 2010.

[6] W. K. Kim, S. B. Park, and S. A. Johnson, "Signal-to-noise ratio and band with for preudo-random codes in an ultrasonic imaging system," *SAGE Ultrasonic Imaging*, vol. 6, pp. 113-123, July1984.

[7] H. Furuhashi, Y. Kuzuya, and M. Shimizu, "Imaging Sensor System Using a Composite Ultrasonic Array," *Proceedings of IEEE SENSORS*, pp. 1467-1472, Oct. 2009.

[8] S. Kumar, K. Ichi, and H. Furuhashi, "Theoretical investigation of high-power ultrasonic array transmitter for a range sensor in air," *Proceedings of IEEE International Conference on Industrial Technology* (*ICIT*), pp. 1190-1195, Feb. 2013.

[9] S. Kumar, and H. Furuhashi, "Long-range measurement system using ultrasonic range sensor with high-power transmitter array in air," *ELSEVIER Ultrasonics*, vol.74, pp. 186-195, Feb. 2017.

[10] G. Allevato, J. Hinrichs, D. Grosskurth, M. Rutsch, J. Adler, A. Jager, M. Pesavento, and M. Kupnik, "3D imaging method for an air-coupled 40kHz ultrasound phased-array," *Proceedings of ICA Internationall Congress on Acoustic*, pp. 4775-4782, Sep. 2019.

[11] L. Segers, J. Tiete, and A. Thouhafi, "Ultrasonic Multiple-Access Ranging System Using Spread Spectrum and MEMS Technology for Indoor Localization," *MDPI Sensors*, vol. 14, no. 2, pp. 3172-3187, Feb. 2014.

[12] T. Ishii, Y. Yoshikawa, S. Izumi, and H, Kawaguchi, "Doppler shift compensisation technique for ultrasonic DSSS ranging system," *Proceedings of IEEE International Instrumentation and Measurement Technology Conference* (*I2MTC*), pp. 1-6, May 2020.